Journal of Catalysis 258 (2008) 44–51

Contents lists available at ScienceDirect

Journal of Catalysis

www.elsevier.com/locate/jcat

Dimer saddle point searches to determine the reactivity of formate on Cu(111)

Donghai Mei [a,*], Lijun Xu [b], Graeme Henkelman [b,*]

[a] Institute of Interfacial Catalysis, Chemical and Materials Sciences Division, Pacific Northwest National Laboratory, P.O. Box 999, K1-83, Richland, WA 99352, USA
[b] Department of Chemistry and Biochemistry, University of Texas at Austin, 1 University Station A5300, Austin, TX 78712, USA

ARTICLE INFO

Article history:
Received 26 February 2008
Revised 13 May 2008
Accepted 23 May 2008
Available online 2 July 2008

Keywords:
Reactivity
Density functional theory
Dimer method
Cu(111)
Formate

ABSTRACT

We used the dimer saddle point searching method with density functional theory calculations to study the reactivity of formate (HCOO) on the Cu(111) surface. We identified possible reaction paths for the HCOO decomposition (or synthesis) and hydrogenation in the presence of a co-adsorbed H atom without assuming their final states. Starting from the most stable bidentate HCOO adsorption configuration, we calculated the pre-exponential factors and reaction rates of the identified HCOO reaction and diffusion paths using harmonic transition state theory. In agreement with previous experimental and theoretical studies, we found that HCOO was formed by gaseous CO_2 and adsorbed H through the Eley–Rideal (ER) mechanism. The activation barriers for direct HCOO synthesis from CO via the ER and Langmuir–Hinshelwood (LH) mechanisms were 1.44 and 2.45 eV, respectively, suggesting that the reaction pathways CO or CO(g) + OH ↔ HCOO were unfavorable on the Cu(111) surface. The decomposition of HCOO to HCO + O was much slower than its reverse recombination. This indicated that the reaction pathway from HCOO to HCO also was unlikely. On the other hand, the reaction route for HCOO hydrogenation to H_2COO in the presence of a co-adsorbed H atom had an activation energy of 1.24 eV, suggesting that HCOO hydrogenation was competitive with HCOO decomposition via the ER mechanism with a barrier of 1.30 eV. Except for two fast HCOO diffusion processes, our results showed that HCOO ↔ CO_2(g) + H and HCOO + H ↔ H_2COO were the dominant reaction pathways on the Cu(111) surface.

1. Introduction

One of the most challenging problems in heterogeneous catalysis is identifying reaction mechanisms without relying primarily on chemical intuition. The mechanism of a heterogeneous catalytic reaction generally involves a series of elementary reactions and diffusion steps. Finding the dominant elementary reaction and diffusion paths and calculating the rates of these elementary steps are vital not only to the fundamental understanding of the chemistry of complex catalytic reaction, but also to the elucidation and prediction of reaction kinetics under reaction conditions. Unfortunately, due to the limitations of current experimental techniques, our knowledge of the reaction mechanism is often incomplete and a matter of debate. The reactivity and kinetic behavior of the same reaction differ greatly under different reaction conditions and catalyst preparation methods. A set of "reasonable" assumptions usually is used to construct a reaction mechanism that explains experimental observations. Over the past 20 years, quantum chemistry density functional theory (DFT) calculations have widely been used to study the reactivity and the energetics of the individual elementary steps of catalytic reactions on metal and metal oxide catalyst surfaces [1]; however, information on the reaction mechanism provided by these DFT calculations remains limited, because most DFT calculations are based on assumed reactants, products, and reaction intermediates. In most cases, a well-designed elementary reaction path, including the most stable or possible configurations of the initial reaction state and the final product state, is determined a priori before the transition state is identified. In this work, we demonstrate that combining standard DFT calculations with the "dimer" saddle point searching method [2] allows us to find the important reaction mechanisms and the corresponding reaction rates of a molecule on a catalyst surface without previous knowledge of the final state.

Formate (HCOO) is considered one of the important surface intermediates in methanol synthesis over $Cu/ZnO/Al_2O_3$ catalysts from syngas ($CO_2/CO/H_2$) [3]. Most previous experimental studies have suggested that the bidentate HCOO species was formed from CO_2 hydrogenation on metallic Cu surfaces [4,5]. CO is not directly involved in HCOO formation, but is involved in the accompanying water–gas shift reaction [6,7]. HCOO is further hydrogenated into methoxy and finally to form methanol. The hydrogenation of HCOO is assumed to be the rate-determining step in methanol synthesis on Cu surfaces [8–12]. The adsorption and the reactivity of HCOO on Cu(111) surface were extensively studied by Nakamura's

* Corresponding authors. Faxes: +1 (509) 375 4381 (D. Mei), +1 (512) 471 4179 (G. Henkelman).
E-mail addresses: donghai.mei@pnl.gov (D. Mei), henkelman@mail.utexas.edu (G. Henkelman).

0021-9517/$ – see front matter
doi:10.1016/j.jcat.2008.05.024

group [4,5,13–15], who found that HCOO adsorbed on the Cu(111) surface in a bridging bidentate structure. In this adsorption configuration, two O atoms of HCOO bonded with two atop Cu atoms. The saturation coverage of HCOO was estimated to be 0.24 ML (1 ML indicating one HCOO molecule per Cu surface atom) using scanning tunneling microscopy and X-ray photoelectron spectroscopy (XPS) [16]. The activation barrier of HCOO synthesis from CO_2 and H_2 was measured as 0.57 eV by XPS [5] and 0.59 eV by *in situ* infrared reflection absorption (IRAS) in the temperature range of 323–353 K; the rate at 353 K was measured at 9.09×10^{-4} molecules site^{-1} s^{-1} [14]. First-order kinetics for HCOO decomposition was found with a measured activation barrier of 1.17 eV by XPS [5] and 1.12 eV by IRAS [14], and a pre-exponential factor of 1.87×10^{11} s^{-1}.

Compared with the aforementioned experiments, only a few theoretical studies of HCOO adsorption and reactivity on Cu surfaces have been reported to date [17–22]. Wang et al. investigated the structure sensitivity of HCOO synthesis and decomposition on Cu(111), Cu(100), and Cu(110) surfaces using periodic DFT calculations [22]. A bidentate HCOO structure was found to be the most stable adsorption structure on Cu surfaces. They reported that HCOO formed on three low-index single crystal Cu surfaces, from CO_2 and H_2 via the Eley–Rideal (ER) mechanism, through an unstable monodentate HCOO structure bound at the 3-fold hollow site. The insensitivity of HCOO synthesis to the surface structure had been explained by the formation of the unstable monodentate HCOO structure, which was found to have similar activation energy on different Cu surfaces. However, the decomposition of the stable bidentate HCOO was sensitive to the Cu surface structure [22]. The calculated activation barriers for HCOO synthesis were 0.69 eV on Cu(111) and 0.64 eV on Cu(110), whereas the barriers for HCOO decomposition were 0.97 eV on Cu(111) and 1.44 eV on Cu(110) [22]. Hu et al. studied methanol synthesis from CO_2 hydrogenation on Cu(100) using the dipped adcluster model combined with *ab initio* Hartree–Fock and second-order Moller–Plesset (MP2) [21], and found that HCOO was formed via the Langmuir–Hinshelwood (LH) mechanism by co-adsorbed CO_2 and H. The activation barrier for HCOO synthesis was found to be 0.53 eV, which is close to that on the Cu(111) surface [22]. The HCOO decomposition on Cu(100) was 1.76 eV [21], demonstrating again that the reactivity of HCOO decomposition is sensitive to the structure of the Cu surface. Hu et al. also showed that the HCOO hydrogenation to dioxomethylene (H_2COO) step on Cu(100) is the rate-limiting step because it had the highest activation barrier (~1.0 eV) of all elementary steps from CO_2 hydrogenation to methanol [21]. Gomes investigated different HCOO adsorption configurations on Cu surfaces using cluster model DFT calculations [18] and found that a short-bridge (bidentate) structure of HCOO was the most stable adsorption configuration.

In this paper we present a computational methodology that provides a valuable tool for studying catalytic reaction mechanisms. We have investigated the reactivity of HCOO on the Cu(111) surface using DFT calculations combined with the dimer method [2,23,24]. The paper is organized as follows. In Section 2, we give a brief description of the computational methodology. In Section 3, we define one of the stable adsorption configuration of HCOO on the Cu(111) surface as the initial state. Starting from this initial state, we identify different pathways of HCOO decomposition (and the reverse path, HCOO synthesis) and hydrogenation in the presence of a co-adsorbed H atom, without knowledge of the final states. Finally, we summarize our results and conclude in Section 4.

2. Computational details

First-principles periodic DFT calculations combined with minimum-mode following saddle point searches were carried out to explore the reaction and diffusion pathways of HCOO on the Cu(111) surface. These plane-wave DFT calculations were performed using the Vienna *ab initio* simulation package [25,26]. The projector augmented wave method with a frozen-core approximation was used to describe the ion–electron interactions. A cutoff energy of 400 eV and the generalized gradient approximation with the Perdew–Burke–Ernzehof functional was used in the calculations. The ground-state atomic geometries of bulk and surfaces were obtained by minimizing the Hellman–Feynman forces with the conjugate-gradient algorithm until the total force on each ion dropped below 0.001 eV/Å. The Cu(111)-3×3 surface was modeled with a three-layer slab, subject to three-dimensional periodic boundary conditions. The slab was separated from its image in the z-direction, perpendicular to the x–y surface plane by a 10 Å vacuum. The bottom two atomic layers were fixed at equilibrium bulk positions, while all the other atoms were allowed to relax. A $2 \times 2 \times 1$ Monkhorst–Pack k-point sampling of the Brillouin zone was used.

The binding energies, E_b, of HCOO on the surface were calculated by the following equation:

$$E_b = E_{HCOO+Cu(111)} - (E_{HCOO} + E_{Cu(111)}), \quad (1)$$

where $E_{HCOO+Cu(111)}$ is the total energy of the interacting system of Cu(111) slab and HCOO molecule; $E_{Cu(111)}$ is the total energy of the bare Cu(111) slab, and E_{HCOO} is the energy of one HCOO molecule in the vacuum. Negative E_b values indicate favorable (exothermic) adsorption.

The minimum-mode following dimer method was used to find saddle points (transition states) from initial minima, without previous knowledge of the possible final states. This method has been described in detail elsewhere [2,23,24], and we give just a brief description here. First, the most stable configuration of the reactant molecule on the surface is determined with a standard DFT minimization. This configuration is used as the initial state. Searches are initiated by displacing the atoms in the reactant molecule by a Gaussian-distributed random distance of 0.05 Å. From this configuration, a dimer is created by making two equal and opposite finite-difference displacements in the coordinates of the reactant molecule. A nearby saddle point is then found iteratively, alternatively taking rotation and translation steps. In the rotation step, the lowest curvature direction is found by minimizing the energy of the dimer with respect to its orientation. In the translation step, the force at the center of the dimer is inverted along the dimer orientation, so that it points up the potential along the lowest curvature mode and down in all other directions. Both rotation and translation steps are implemented with a conjugate gradient optimizer. A one-sided (forward difference) dimer method is used to reduce the total number of force evaluations needed [24,27]. All saddle points identified in this work were confirmed to be first-order saddles using a finite-difference normal mode analysis; only one imaginary frequency was obtained at each saddle point.

After each saddle point is found, the dimer images are displaced from the saddle along the negative mode by 0.1 Å and then relaxed to the neighboring local minima. In a successful search, one of the images will minimize to the initial state, and the other will be in a new (and perhaps surprising) final state. In this work, the dimer separation was set at 0.0l Å, and the tolerance for convergence to the transition state was such that the force on each atom was less than 0.005 eV/Å. The reaction energy of each path is calculated as the total energy difference between the final state and the initial state. The forward and reverse activation barriers of each reaction (diffusion) path are defined as the total energy difference between

the initial state and the saddle point and between the final state and the saddle point, respectively.

3. Results and discussion

3.1. Determination of initial state

In the present study, only the initial state (i.e., the stable HCOO adsorption state) was a prerequisite for exploring the reaction and diffusion pathways of HCOO on the Cu(111) surface. Much experimental evidence suggests that the adsorbed HCOO species is in a bidentate configuration [4,5,13–16], in which both O atoms of the HCOO molecule bind atop Cu atoms on the surface with the HCOO molecular plane perpendicular to the (111) direction. This bridging bidentate HCOO molecule is positioned on a Cu(111)-3 × 3 surface in our initial state. The HCOO coverage in the initial state is 1/9 ML, which is a relevant coverage for catalysis [4,16]. The optimized bidentate HCOO structure is shown in Fig. 1a. The calculated Cu–O distance of 2.01 Å is consistent with all known μ_2-formate–copper complexes (1.98 ± 0.04 Å) and the reported experimental value of 1.92 ± 0.04 Å using normal incidence X-ray standing wavefield absorption (NIXSW) [28], as well as with previous DFT cluster model calculations with the B3LYP hybrid functional (2.015 Å) [18]. Our calculated O–C–O angle of 126.9° also is very close to the previously reported value of 127.8° [18]. In agreement with previous experimental findings [28], no noticeably structural perturbation of the Cu(111) surface occurred after HCOO adsorption. The binding energy of the bidentate HCOO of −3.31 eV is similar to the previous cluster model DFT result of −3.41 eV [18].

3.2. Diffusion pathways

Starting with the stable bidentate HCOO adsorption configuration, two more stable adsorption structures of HCOO were found with our saddle point searches and the subsequent identification of two diffusion pathways. Similar to the bridging bidentate structure, HCOO also was bound at a 3-fold hollow site on the Cu(111) surface. For bidentate HCOO at the 3-fold hollow site shown in Fig. 1b, one O atom of HCOO was bridge-bound with two surface Cu atoms and the other O atom was bound atop the third surface Cu atom. The two equal bridging Cu–O bond lengths were 2.22 Å, longer than the single Cu–O bond in the bridging bidentate structure. The binding energy for the bidentate HCOO bound at the 3-fold hollow site of −3.06 eV is slightly weaker than that of the most stable bridging bidentate structure. Of note is the unusual diffusion path for the bidentate HCOO from the bridge site to the hollow site. The diffusion path is not a direct tilting of the bidentate HCOO from the bridge site to the neighboring hollow site, but rather occurs by "walking" to the next-neighboring hollow site. As shown in Fig. 2a, the saddle point of this diffusion path has two O atoms of HCOO binding at two next-neighboring Cu atoms on the (111) surface. One O atom of the HCOO molecule "walks" from the one Cu atom to another next-neighboring Cu atom, while the other O atom remains bound at the original Cu atom. Consequently, both Cu–O bonds are elongated to 2.13 Å at the saddle point. The two bonded Cu atoms have been pulled out of the surface plane by 0.14 Å. The forward and reverse barriers of this diffusion path are 0.39 eV and 0.29 eV, respectively.

HCOO can adsorb on the Cu(111) surface in a monodentate structure, in which only one O atom binds with the surface. Similar to the previously reported monodentate HCOO structure [22], we found the monodentate HCOO adsorbs at a 3-fold hollow site on the Cu(111) surface with the binding energy of −2.68 eV. Compared with the two bidentate structures mentioned above, the monodentate HCOO adsorption is weak. As shown in Fig. 1c, the Cu–O bonds have been slightly elongated to 2.08–2.13 Å in the

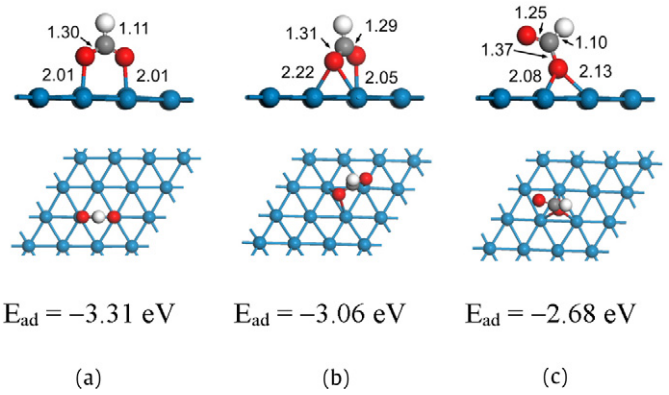

Fig. 1. Adsorption of HCOO on the Cu(111) surface. (a) Bidentate HCOO at bridge site; (b) bidentate HCOO at hollow site; (c) monodentate HCOO at hollow site. The numbers in the figure are the bond distances in optimized structures. Cu atom is in blue, O atom in red; C atom in gray and H atom in white. The same color scheme is applied in all figures. (For interpretation of the references to color in this figure legend, the reader is referred to the web version of this article.)

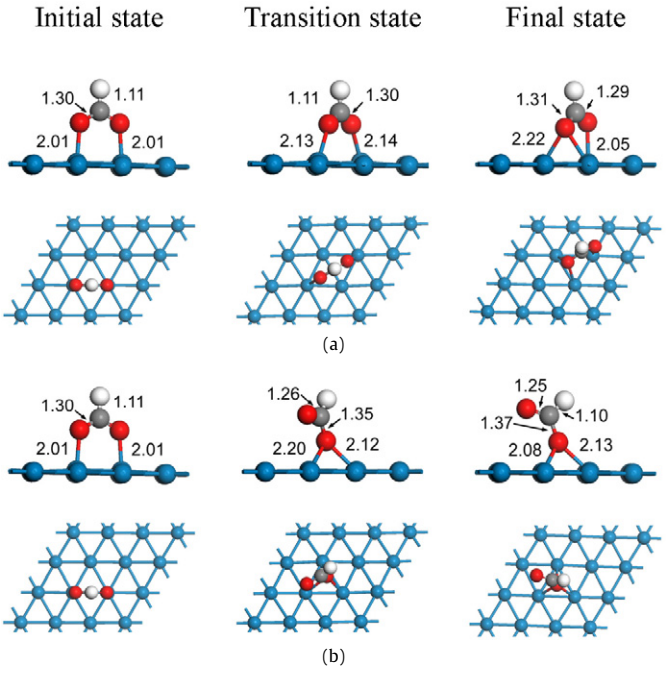

Fig. 2. HCOO diffusion paths. (a) Bidentate HCOO from the bridge site to the hollow site; (b) bidentate HCOO from the bridge site to monodentate at the hollow site.

monodentate configuration. In contrast, the two C–O bonds of the adsorbed HCOO molecule become unequal (1.37 and 1.25 Å). The forward and reverse diffusion barriers of HCOO from the bridging bidentate to the 3-fold hollow monodentate are 0.46 and 0.02 eV, respectively, indicating that the monodentate HCOO at the hollow site is unstable and readily migrates to the bidentate configuration at the bridge site on the Cu(111) surface. The saddle point of this diffusion path, shown in Fig. 2b, has a late transition state, because the geometries and energies of both transition state and final monodentate state are nearly the same.

The monodentate HCOO adsorption at the atop site on the Cu(111) surface was not found in our dimer calculations. A separate DFT calculation showed that the monodentate HCOO at the atop site was unstable and always shifted to a bidentate structure at the bridge site after structural optimization. Because the diffusion barrier from the monodentate HCOO to the bidentate HCOO

is only 0.02 eV, the monodentate HCOO at 3-fold hollow site will quickly transform to the bridging bidentate structure if the bridge site is available at low surface coverage.

To summarize, we found three stable adsorption configurations for HCOO on the Cu(111) and two diffusion pathways. Initial guesses based on chemical or physical intuitions are not necessary to find all possible adsorption configurations of the reactant on the catalyst surface when using the combined methodology of DFT and dimer saddle point searches.

3.3. Reaction pathways

3.3.1. HCOO decomposition

3.3.1.1. HCOO ↔ CO_2(g) + H The first HCOO decomposition path has HCOO decomposing into an adsorbed H atom on the surface and a CO_2 molecule into the gas phase, that is, an ER decomposition mechanism. The initial state is the bridging bidentate HCOO, which is shown in Fig. 3a. The transition and final states are also shown in Fig. 3a. Before the transition state, the bidentate HCOO moves from the stable bridge site to the hollow site with the monodentate structure. At the transition state, the C–H bond is already broken, because the distance between C and H atom is 1.66 Å. Here the CO_2 molecule still binds at the atop site with a single Cu–O bond, whereas the H atom binds at the bridge site on the Cu(111) surface. In the final state, the CO_2 molecule desorbs from the surface, and the adsorbed H atom moves from the bridge site to the most stable hollow site. The activation barrier and reaction energy of HCOO ↔ CO_2(g) + H is 1.30 and +0.73 eV. Nakamura et al. studied the decomposition and synthesis kinetics of HCOO on Cu(111) using XPS and IRAS techniques [5,14]. The activation energies for HCOO decomposition to CO_2 + H_2 were found to be 1.17 ± 0.13 eV by XPS [5] and 1.12 ± 0.03 eV by IRAS [14]. Our calculation result is in good agreement with the experimental results. A lower activation barrier (0.97 eV) of HCOO decomposition on Cu(111) surface was reported by Wang et al. [22]; our calculation yielded the same conclusion, that the ER mechanism is the only mechanism for HCOO decomposition to CO_2 and H, whereas it did not identify the LH mechanism. This suggests a very weak interaction of CO_2 with the Cu(111) surface. The binding energy of CO_2 at the atop site was calculated to be only 0.03 eV [29].

The reverse reaction path of the foregoing HCOO decomposition path is HCOO synthesis from CO_2 and H_2. This path had been considered the first step in methanol synthesis from CO_2 hydrogenation. The activation barrier for the ER mechanism of HCOO formation on the Cu(111) surface of 0.57 eV is in excellent agreement with the experimentally determined HCOO synthesis barriers of 0.57 ± 0.06 eV by XPS [5] and 0.59 ± 0.05 eV by IRAS [14]. A slightly higher barrier of 0.69 eV was reported by Wang et al. [22].

Although two bidentate HCOO structures (at the bridge and hollow sites) are more stable on the Cu(111) surface, the monodentate HCOO structure at the hollow site is an intermediate structure (or precursor state) for HCOO decomposition or synthesis via a ER mechanism. The bidentate HCOO is not formed directly from CO_2(g) reacting with surface H atoms, but rather is formed through a metastable monodentate HCOO configuration. Similar to previous findings [22], our calculations confirm that the metastable monodentate HCOO state bound at the 3-fold hollow site exists in HCOO synthesis and decomposition pathways on the Cu(111) surface.

3.3.1.2. HCOO ↔ CO(g) + OH and HCOO ↔ CO + OH Both the ER and LH reaction paths were found for HCOO decomposition into CO and OH. HCOO decomposes either into adsorbed OH and CO in the gas phase or into co-adsorbed CO and OH on the surface. Here we first discuss the ER mechanism of HCOO decomposition to CO and

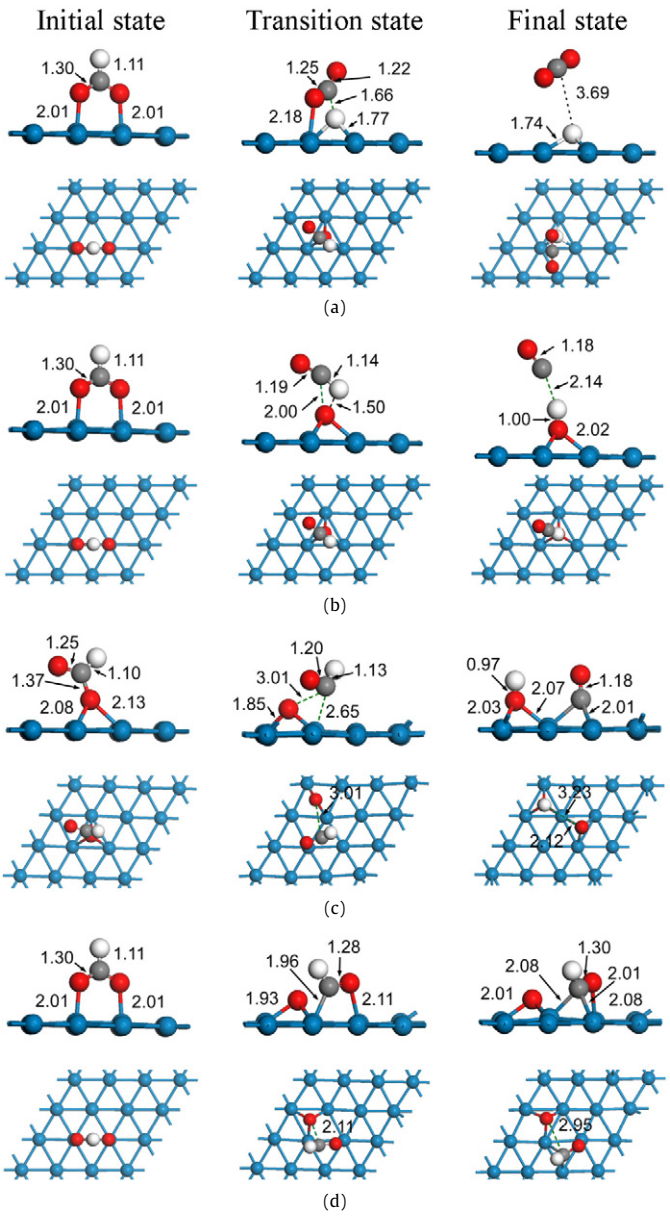

Fig. 3. HCOO decomposition pathways. (a) HCOO ↔ CO_2(g) + H; (b) HCOO ↔ CO(g) + OH; (c) HCOO ↔ CO + OH; (d) HCOO ↔ HCO + O.

OH. The bidentate HCOO adsorbed at the bridge site on the Cu(111) is the initial state. The transition and final states of this identified path are shown in Fig. 3b. The bidentate HCOO must move to the hollow site in the monodentate configuration. At the transition state, one of the C–O bonds of HCOO molecule is broken. The distance between the C atom and the surface bonded O atom is 2.00 Å. The dissociated HCO fragment is lifted up from the surface. Each atom of the HCO fragment also rotates in the plane normal to the surface and rearranges itself into the linear HCO configuration. Simultaneously, the H atom of HCOO moves close to the surface bonded O atom. The distance between the H atom and the surface bonded O atom of HCOO is 1.50 Å. The C–H bond length of HCOO is 1.14 Å at the transition state, slightly longer than the normal C–H bond length of 1.11 Å in the stable bidentate HCOO structure. This suggests that the C–H bond of HCOO has not yet ruptured at the transition state. In the final state, the C–H bond is broken, as the distance between the C and H atoms increases to 2.14 Å. The H atom recombines with the surface-bonded O atom to form an OH group on the surface, and the CO molecule is released into the

gas phase. This reaction path is highly endothermic. The calculated reaction energy for HCOO ↔ CO(g) + OH is 1.36 eV. A high activation barrier of 2.80 eV is obtained.

We also identified the decomposition of HCOO into CO and OH via a LH surface mechanism. Similar to the aforementioned ER mechanism, one of the C–O bonds is broken at the transition state; however, the O atom is bonded at the bridge site instead of at the hollow site in the transition state. The broken C–O bond distance is 3.01 Å. As shown in Fig. 3c, the HCO fragment is lifted up away from the surface but remains in a nonlinear configuration, different from the linear configuration in the ER mechanism. The C–H bond is slightly elongated from 1.11 to 1.13 Å. The distance between the C atom and the closest surface Cu atom is 2.65 Å. After the transition state, the C–H bond of the HCO fragment is broken. The H atom moves toward the bonded O atom, forming an OH group at the hollow site. The CO molecule also moves down and eventually binds at the neighboring hollow site on the surface. Compared with the ER mechanism, this LH mechanism is less endothermic. The calculated reaction energy for HCOO ↔ CO + OH is 0.56 eV; however, the activation barrier of HCOO ↔ CO + OH is 3.01 eV, 0.21 eV higher than that of ER mechanism decomposition path.

3.3.1.3. HCOO ↔ HCO + O The fourth decomposition path for HCOO that we found is the dissociation of HCOO into a formyl (HCO) species and an O atom. The transition and final states of this reaction path are shown in Fig. 3d. At the transition state, one of the O atoms of HCOO moves from the atop site to the hollow site, breaking the C–O bond. At the same time, the C atom of HCOO replaces the moving O atom and binds at the original atop site. The dissociated HCO fragment binds at the bridge site. The Cu–C and Cu–O bond lengths of HCO at the bridge site are 2.01 and 2.08 Å, respectively. In the final state, HCO moves from the bridge site to the most stable hollow site. This decomposition path is also endothermic, with a reaction energy of 1.40 eV. The calculated activation barrier for HCOO ↔ HCO + O is 1.70 eV.

3.3.2. Comparison of HCOO decomposition paths

We have identified four different reaction paths for HCOO decomposition. It is interesting to compare the reaction rates of these four decomposition reaction paths. The reaction rate r_i of each path (both forward and reverse) is calculated using harmonic transition state theory [30,31],

$$r_i = \nu_i \cdot \exp\left(\frac{-E_a^{\neq}}{RT}\right), \tag{2}$$

where ν_i is the pre-exponential factor and $E_a^{\neq}$ is the activation barrier. Based on harmonic transition-state theory, we can calculate the pre-exponential factors (ν_i) of each reaction pathway using the following definition:

$$\nu_i = \frac{\prod_1^{3N} f_i^{IS}}{\prod_1^{3N-1} f_i^{TS}}, \tag{3}$$

where f_i^{IS} are the vibrational frequencies at the initial state and f_i^{TS} are the vibrational frequencies at the transition (excluding the imaginary one). For the reverse pathway, we used f_i^{FS}, the vibrational frequencies at the final state, instead of f_i^{IS} in Eq. (3). We also investigated the effect of the zero-point energy correction (ZPEC) on the reaction energies and the activation barriers. Table 1 listed the calculated pre-exponential factors along with the activation barriers with and without ZPEC. We found that ZPEC had only a slight effect on the calculated energetics in this work (<0.1 eV).

Compared with experimental estimation of the pre-exponential factors, our calculated values are larger. For example, For HCOO ↔ CO_2(g) + H, the calculated pre-exponential factor of 1.98 ×

Table 1
Calculated activation barriers $E^{\neq}$ (eV), the pre-exponential factors ν (s^{-1}), and the rate constants k (s^{-1}) of HCOO reaction and diffusion pathways

	$\nu_{forward}$	$\nu_{reverse}$	Without ZPEC		With ZPEC		$T = 353$ K		$T = 403$ K	
			$E^{\neq}_{forward}$	$E^{\neq}_{reverse}$	$E^{\neq}_{forward}$	$E^{\neq}_{reverse}$	$k_{forward}$	$k_{reverse}$	$k_{forward}$	$k_{reverse}$
HCOO(bi) ↔ CO_2(g) + H	1.98×10^{14}		1.30	0.57	1.25	0.56	5.4×10^{-5}		1.1×10^{-2}	
HCOO(bi) ↔ CO(g) + OH	1.56×10^{16}		2.80	1.44	2.72	1.43	1.6×10^{-24}		1.5×10^{-19}	
HCOO(bi) ↔ CO + OH	2.46×10^{14}	4.90×10^{12}	3.01	2.45	2.97	2.45	2.6×10^{-29}	5.1×10^{-23}	5.6×10^{-24}	1.1×10^{-18}
HCOO(bi) ↔ HCO + O	1.84×10^{12}	5.89×10^{12}	1.70	0.30	1.64	0.29	9.8×10^{-13}	3.1×10^{8}	1.0×10^{-9}	1.0×10^{9}
HCOO(bi) + H ↔ H_2COO	5.88×10^{12}	1.50×10^{14}	1.24	0.85	1.14	0.76	1.2×10^{-5}	1.1×10^{2}	1.8×10^{-3}	3.5×10^{3}
HCOO(bi) ↔ HCOO(mono)	1.52×10^{13}	1.56×10^{12}	0.46	0.02	0.44	0.02	4.1×10^{6}	8.1×10^{11}	2.7×10^{7}	8.8×10^{11}
HCOO(bi) ↔ HCOO(hollow)	2.12×10^{13}	1.46×10^{13}	0.39	0.28	0.38	0.27	5.7×10^{7}	1.5×10^{9}	2.8×10^{8}	4.6×10^{9}

Note. The activation barriers without ZPEC were used in the calculations of the rate constants at 353 and 403 K.

10^{14} s^{-1} is larger than the experimentally estimated value of 1.87×10^{11} s^{-1} [14]. This high calculated pre-exponential factor is expected for the desorption reaction, because entropy increases as the CO_2 molecule leaves the surface. There could also be some uncertainty in the experimental barrier and prefactor; determining these parameters individually is difficult unless the experiments are done over a wide temperature range. This is likely, because at 373 K, our calculated reaction rate is 5.4×10^{-4} s^{-1}, which is close to the experimental estimation of 1.50×10^{-4} s^{-1} [15].

Table 1 also gives the calculated reaction rates of different HCOO decomposition and synthesis pathways at 353 and 403 K. For HCOO synthesis, clearly the ER mechanism in which CO_2 directly reacts with the adsorbed H on the Cu(111) surface is the major pathway for HCOO synthesis. In agreement with previous experimental observations, our reaction rate calculations indicate that a direct CO hydrogenation path (ER or LH mechanism) in methanol synthesis from syngas containing CO_2, CO, and H_2 is not feasible on the Cu(111) surface. On the other hand, as the temperature increases from 353 to 403 K, the HCOO decomposition rate (to CO_2 and H) increases by a factor of 200, whereas the HCOO synthesis rate (the reverse path) remains nearly constant. This suggests that HCOO formation is favored at low temperature. In addition, HCOO decomposition into HCO and O is much slower than decomposition to CO_2 and H in the temperature range studied.

3.3.3. *Hydrogenation of HCOO: HCOO + H ↔ H_2COO*

The role of HCOO in methanol synthesis on Cu-based catalysts remains under debate. Although most experimental and theoretical studies assume that HCOO is a surface intermediate in the methanol synthesis route from CO_2 + H_2, there is no indisputable experimental evidence of HCOO hydrogenation on metallic Cu surfaces. In line with previous experimental observations [5,11,15,32–36], our calculations show that HCOO is formed from CO_2 and adsorbed H on the Cu(111) surface via the ER mechanism. If HCOO is a key reaction intermediate in methanol synthesis on Cu catalysts, the HCOO formed must be further hydrogenated into methoxy (H_3CO) and then into methanol. Wachs and Madix studied the oxidation of formaldehyde (H_2CO) on Cu(110) using temperature-programmed reaction spectroscopy (TPRS) [37] and found dioxymethylene (H_2COO) during the transformation of H_2CO to HCOO. H_2CO reacts with a preadsorbed surface O atom to form H_2COO on the surface. H_2COO then quickly dehydrogenates to HCOO and eventually to CO_2 and H_2 [37]. H_2COO also was observed in methanol decomposition on Cu/SiO_2 and $Cu/ZnO/Al_2O_3$ using TPRS and NMR techniques [38,39]. Burch et al. proposed that the first hydrogenation step of HCOO into H_2COO was the critical rate-determining step in methanol synthesis on Cu surfaces [11]; however, Sexton et al. claimed that there was no clear evidence of the existence of H_2COO in their study of methanol and H_2CO reaction on the Cu(110) surface [40]. The inconsistency of experimental observations on the possible H_2COO surface intermediates during the consecutive hydrogenation steps in methanol synthesis may be due to the short lifetime of H_2COO on Cu surfaces. It is possible that the H_2COO intermediate either quickly dissociates back to HCOO or forms H_2CO by reacting with a neighboring H or hydroxyl group.

To clarify this important question of whether the hydrogenation of HCOO to H_2COO on Cu surfaces is important, we calculated the HCOO hydrogenation on the Cu(111) surface. In the initial state, shown in Fig. 4a, the most stable bridging bidentate HCOO coadsorbs with an H atom at the neighboring 3-fold hollow site. To avoid any artificial interaction between periodic images, the distance between the co-adsorbed HCOO and H atom is set far enough (4.04 Å) to minimize possible lateral interactions. At the initial state, the calculated interaction between adsorbed HCOO and H atom is negligibly repulsive (0.09 eV) [29]. The reaction path of HCOO hydrogenation to H_2COO shown in Fig. 4 has been identified in this work. At the transition state, shown in Fig. 4b, the HCOO molecule tilts toward the surface H atom, and the adsorbed H atom moves from the most stable hollow site to the bridge site. As a result, the distance between the C atom of HCOO and H atom decreases from 4.04 Å at the initial state to 1.55 Å at the transition state. During this transformation, both Cu–O bond lengths of HCOO are elongated from 2.01 Å at the initial state to 2.14 Å at the transition state. At the final state, shown in Fig. 4c, H_2COO adsorbs on the surface with both O atoms bonded at two parallel bridge sites. The calculated activation barrier of HCOO hydrogenation to H_2COO is 1.24 eV. This hydrogenation reaction path is endothermic, with a reaction energy of 0.39 eV.

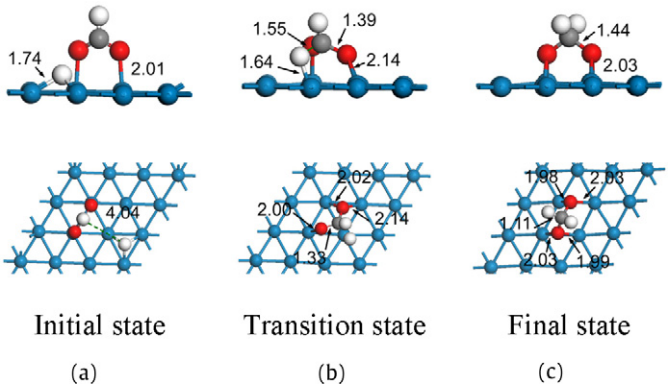

Fig. 4. HCOO hydrogenation to H_2COO.

Compared with the activation barrier of HCOO decomposition (to CO_2) via the ER mechanism, we found a similar barrier for HCOO hydrogenation (to H_2COO). This suggests that H_2COO is a possible reaction intermediate in the presence of co-adsorbed HCOO and H. We identified the H_2COO species without presuming its existence. HCOO hydrogenation to H_2COO is a feasible step on the Cu(111) surface, the predominant surface in Cu catalysts. Using Eq. (3), we obtained pre-exponential factors of 5.88×10^{12} s^{-1} for HCOO hydrogenation and 1.50×10^{14} s^{-1} for HCOO dehydrogenation. As shown in Table 1, the calculated reaction rate of HCOO hydrogenation is 5–6 times slower than that of HCOO decomposition to CO_2 in the temperature range of 353–403 K even though the hydrogenation barrier is slightly lower. Comparing the reaction rates of HCOO decomposition and hydrogenation indicates that HCOO may decompose before hydrogenation even in the presence of adsorbed H on the surface. On the other hand, the dehydrogenation rate of H_2COO to HCOO is about 2×10^6–10^7 times greater than the HCOO hydrogenation rate. Once H_2COO is formed, it can be easily dehydrogenated back to HCOO before further oxydehydronation to H_2CO and H_3CO occurs. The formation of H_2COO may be the rate-determining step in the route of HCOO hydrogenation to methanol on the Cu(111) surface. Hu et al. [21] calculated the activation barrier of HCOO hydrogenation to H_2COO on Cu(100) surface using the *ab initio* Hartree–Fock method with the dipped adcluster model. Similar to our results, the activation barrier for HCOO hydrogenation was about 1.00 eV, and the total reaction energy was endothermic (0.74 eV) [21]. They also found that the barrier for HCOO hydrogenation was larger than the barriers of HCOO formation (0.53 eV) and H_2COO hydrogenation (0.74 eV). Based on these findings, they proposed that the HCOO hydrogenation to H_2COO may be the rate-controlling step in methanol synthesis from CO_2 hydrogenation on the Cu(100) surface. Because we have not totally explored the reactivity of H_2COO on the Cu(111) surface using the method reported here, we can only conclude that HCOO hydrogenation is possibly an important step.

Gomes studied the adsorption of H_2COO on the Cu(111) surface using a Cu_{30} cluster model [19]. The most stable adsorption for H_2COO was at the cross-bridge site, with an adsorption energy of −4.30 eV. Our calculated adsorption structure of H_2COO, shown in Fig. 4c, is the same as their structure but with a slightly longer Cu–O bond length (2.03 Å vs 1.96 Å [19]). As noted by Hu and Boyd [20], small cluster models usually overestimate the adsorption energies of HCOO on Cu surfaces. Our calculated binding energy of H_2COO is −3.69 eV, lower than that found by Gomes with this cluster model [19]. Similar to HCOO adsorption, this result suggests that H_2COO binds strongly on the Cu(111) surface. We found the similar bond strengths for H_2COO at the short-bridge site on the Cu(110) and Cu(100) surfaces [29]. The inconsistency of previous experimental observations may be due not to the weak bonding of H_2COO, but rather to the oxydehydrogenation of H_2COO back to HCOO as discussed earlier. Another possible cause may be the mobility of H_2COO on Cu(111); we found that a diffusion barrier of only 0.27 eV for H_2COO rotated 90° at the same Cu–O double-bridge sites [29].

Rate constants depend not only on the activation energy, but also on the pre-exponential factor. Of note, the rationalization of reaction paths in a complex heterogeneous reaction system should be based on the reaction rate constant of each path. Although calculations based on the activation barriers alone may be sufficiently accurate in cases where the pre-exponential factors are nearly the same, in some cases the pre-exponential factors also may be important in determining the important reaction mechanisms, particularly at high temperature. Nakano et al. found that the activation energies for HCOO decomposition on the Cu(111) surface in UHV and in the presence 380 Torr H_2 conditions were almost the same, but the rate constants were different [15]. They suggested that the OCO vibration of HCOO may be responsible for the different decomposition rate constants by changing the pre-exponential factors [15]. In this work, we found that both the activation barriers and the pre-exponential factors are important in determining the rate constants. For example, the activation barrier for HCOO hydrogenation (1.24 eV) is slightly lower than the barrier of HCOO decomposition (1.30 eV). However, the pre-exponential factor of HCOO hydrogenation is 5.88×10^{12} s^{-1}, which is ∼40 times smaller than the pre-exponential factor of HCOO decomposition (1.98×10^{14} s^{-1}). Consequently, the HCOO hydrogenation reaction is 5–6 times slower the HCOO decomposition. Similarly, we found that the activation barrier for H_2COO dehydrogenation is higher than the HCOO formation from CO_2 hydrogenation, but the rate constant of H_2COO dehydrogenation is larger, due to a larger pre-exponential factor.

4. Conclusion

With no knowledge of final states, we have explored the potential energy surface of HCOO on the Cu(111) using periodic DFT calculations combined with the dimer saddle point search method. We have identified four HCOO decomposition (synthesis) pathways, two diffusion pathways, and HCOO hydrogenation forming H_2COO in an unbiased manner. Using harmonic transition-state theory, we also have calculated the rate constants of the identified diffusion and reaction paths. In agreement with experimental results, HCOO was found to decompose into gaseous CO_2 and adsorbed H atom via an ER mechanism. CO hydrogenation to HCOO by recombination with surface OH and its reverse path via both ER and LH mechanisms are unfavorable. The calculated rate constants also suggest that HCOO decomposition into HCO and O is much slower than the HCOO decomposition into CO_2(g) and that the co-adsorbed HCO + O readily forms HCOO by recombination. We identified a H_2COO formation path starting with co-adsorbed HCOO and H. The reaction rate constant of HCOO hydrogenation to H_2COO is comparable to that of the most dominant reaction path, HCOO decomposition to CO_2 via the ER route, indicating that HCOO hydrogenation to H_2COO is a feasible reaction path in methanol synthesis on the Cu(111) surface.

Acknowledgments

This work was supported by a Laboratory Directed Research and Development (LDRD) project of the Pacific Northwest National Laboratory (PNNL). The computations were performed using the Molecular Science Computing Facility in the William R. Wiley Environmental Molecular Sciences Laboratory (EMSL), a U.S. Department of Energy national scientific user facility located at PNNL in Richland, Washington. Computing time was made available through a Computational Grand Challenge, "Computational Catalysis," and user facility allocation EMSL-25428. Some computing time also was provided by the National Energy Research Scientific Computing Center (NERSC). G.H. gratefully acknowledges support from the NSF CAREER program (CHE-0645497), the Advanced Research Program (ITC-ARP-0022), and the Welch Foundation (F-1601).

References

[1] R.A. van Santen, M. Neurock, Molecular Heterogeneous Catalysis: A Conceptual and Computational Approach, Wiley–VCH, Weinheim, 2006.
[2] G. Henkelman, H. Jonsson, J. Chem. Phys. 111 (1999) 7010–7022.
[3] A.Y. Rozovskii, G.I. Lin, Top. Catal. 22 (2003) 137–150.
[4] T. Fujitani, Y. Choi, M. Sano, Y. Kushida, J. Nakamura, J. Phys. Chem. B 104 (2000) 1235–1240.
[5] H. Nishimura, T. Yatsu, T. Fujitani, T. Uchijima, J. Nakamura, J. Mol. Catal. A Chem. 155 (2000) 3–11.
[6] G.C. Chinchen, P.J. Denny, J.R. Jennings, M.S. Spencer, K.C. Waugh, Appl. Catal. 36 (1988) 1–65.
[7] G.C. Chinchen, P.J. Denny, D.G. Parker, M.S. Spencer, D.A. Whan, Appl. Catal. 30 (1987) 333–338.
[8] J. Yoshihara, C.T. Campbell, J. Catal. 161 (1996) 776–782.
[9] J. Yoshihara, S.C. Parker, A. Schafer, C.T. Campbell, Catal. Lett. 31 (1995) 313–324.
[10] M. Bowker, R.A. Hadden, H. Houghton, J.N.K. Hyland, K.C. Waugh, J. Catal. 109 (1988) 263–273.
[11] R. Burch, S.E. Golunski, M.S. Spencer, Catal. Lett. 5 (1990) 55–60.
[12] P.A. Taylor, P.B. Rasmussen, I. Chorkendorff, J. Chem. Soc. Faraday Trans. 91 (1995) 1267–1269.
[13] I. Nakamura, H. Nakano, T. Fujitani, T. Uchijima, J. Nakamura, Surf. Sci. 404 (1998) 92–95.
[14] I. Nakamura, H. Nakano, T. Fujitani, T. Uchijima, J. Nakamura, J. Vac. Sci. Technol. A Vac. Surf. Films 17 (1999) 1592–1595.
[15] H. Nakano, I. Nakamura, T. Fujitani, J. Nakamura, J. Phys. Chem. B 105 (2001) 1355–1365.
[16] J. Nakamura, Y. Kushida, Y. Choi, T. Uchijima, T. Fujitani, J. Vac. Sci. Technol. A Vac. Surf. Films 15 (1997) 1568–1571.
[17] J.R.B. Gomes, J.A.N.F. Gomes, Electrochim. Acta 45 (1999) 653–658.
[18] J.R.B. Gomes, J.A.N.F. Gomes, Surf. Sci. 432 (1999) 279–290.
[19] J.R.B. Gomes, J.A.N.F. Gomes, Surf. Sci. 446 (2000) 283–293.
[20] Z.M. Hu, R.J. Boyd, J. Chem. Phys. 112 (2000) 9562–9568.
[21] Z.M. Hu, K. Takahashi, H. Nakatsuji, Surf. Sci. 442 (1999) 90–106.
[22] G.C. Wang, Y. Morikawa, T. Matsumoto, J. Nakamura, J. Phys. Chem. B 110 (2006) 9–11.
[23] G. Henkelman, H. Jonsson, J. Chem. Phys. 115 (2001) 9657–9666.
[24] R.A. Olsen, G.J. Kroes, G. Henkelman, A. Arnaldsson, H. Jonsson, J. Chem. Phys. 121 (2004) 9776–9792.
[25] G. Kresse, J. Furthmuller, Phys. Rev. B 54 (1996) 11169–11186.
[26] G. Kresse, J. Furthmuller, Comput. Mater. Sci. 6 (1996) 15–50.
[27] A. Heyden, A.T. Bell, F.J. Keil, J. Chem. Phys. 123 (2005).
[28] A. Sotiropoulos, P.K. Milligan, B.C.C. Cowie, M. Kadodwala, Surf. Sci. 444 (2000) 52–60.
[29] D. Mei, unpublished results.
[30] G.H. Vineyard, J. Phys. Chem. Solids 3 (1957) 121–127.
[31] C. Wert, C. Zener, Phys. Rev. 76 (1949) 1169–1175.
[32] R. Burch, S. Chalker, J. Pritchard, J. Chem. Soc. Faraday Trans. 87 (1991) 193–197.
[33] I. Nakamura, T. Fujitani, T. Uchijima, J. Nakamura, J. Vac. Sci. Technol. A Vac. Surf. Films 14 (1996) 1464–1468.
[34] J. Nakamura, I. Nakamura, T. Uchijima, Y. Kanai, T. Watanabe, M. Saito, T. Fujitani, J. Catal. 160 (1996) 65–75.

[35] T. Yatsu, H. Nishimura, T. Fujitani, J. Nakamura, J. Catal. 191 (2000) 423–429.
[36] J. Yoshihara, S.C. Parker, A. Schafer, C.T. Campbell, Abstr. Pap. Am. Chem. Soc. 209 (1995) 207-COLL.
[37] I.E. Wachs, R.J. Madix, Surf. Sci. 84 (1979) 375–386.
[38] D.B. Clarke, D.K. Lee, M.J. Sandoval, A.T. Bell, J. Catal. 150 (1994) 81–93.
[39] N.D. Lazo, D.K. Murray, M.L. Kieke, J.F. Haw, J. Am. Chem. Soc. 114 (1992) 8552–8559.
[40] B.A. Sexton, A.E. Hughes, N.R. Avery, Surf. Sci. 155 (1985) 366–386.